Journal of Plant Physiology 185 (2015) 13–23

Contents lists available at ScienceDirect

Journal of Plant Physiology

journal homepage: www.elsevier.com/locate/jplph

Molecular biology

A proteome map of a quadruple photoreceptor mutant sustains its severe photosynthetic deficient phenotype

Ana Romina Fox[a,1], Maria Laura Barberini[a], Edmundo Leonardo Ploschuk[b], Jorge Prometeo Muschietti[a,c], Maria Agustina Mazzella[a,*]

[a] Instituto de Investigaciones en Ingeniería Genética y Biología Molecular, Dr. Héctor Torres (INGEBI-CONICET), Buenos Aires 1428, Argentina
[b] Cátedra de Cultivos Industriales, Departamento de Producción Vegetal, Facultad de Agronomía, Universidad de Buenos Aires, Buenos Aires 1417, Argentina
[c] Departamento de Biodiversidad y Biología Experimental, Facultad de Ciencias Exactas y Naturales, Universidad de Buenos Aires, Buenos Aires 1428, Argentina

ARTICLE INFO

Article history:
Received 8 February 2015
Received in revised form 20 July 2015
Accepted 20 July 2015
Available online 29 July 2015

Keywords:
Proteome
Arabidopsis
Phytochrome
Cryptochrome
Photosynthesis

ABSTRACT

Light is the environmental factor that most affects plant growth and development through its impact on photomorphogenesis and photosynthesis. A quadruple photoreceptor mutant lacking four of the most important photoreceptors in plants, phytochromes A and B (phyA, phyB) and cryptochromes 1 and 2 (cry1, cry2), is severely affected in terms of growth and development. Previous studies have suggested that in addition to a photomorphogenic disorder, the *phyA phyB cry1 cry2* quadruple mutant might have severe alterations in photosynthetic ability. Here, we investigated the photosynthetic processes altered in the quadruple mutant and performed a proteomic profiling approach to identify some of the proteins involved. The *phyA phyB cry1 cry2* quadruple mutant showed reduced leaf area and total chlorophyll content. Photosynthetic rates at high irradiances were reduced approximately 65% compared to the wild type (WT). Light-saturated photosynthesis and the response of net CO_2 exchange to low and high internal CO_2 concentrations suggest that the levels or activity of the components of the Calvin cycle and electron transport might be reduced in the quadruple mutant. Most of the under-expressed proteins in the *phyA phyB cry1 cry2* quadruple mutant consistently showed a chloroplastic localization, whereas components of the Calvin cycle and light reaction centers were overrepresented. Additionally, Rubisco expression was reduced threefold in the *phyA phyB cry1 cry2* quadruple mutant.

Together, these results highlight the importance of the phytochrome and cryptochrome families in proper autotrophy establishment in plants. They also suggest that an overall limitation in the chlorophyll levels, expression of Rubisco, and enzymes of the Calvin Cycle and electron transport that affect ribulose-1,5-biphosphate (RuBP) regeneration reduced photosynthetic capacity in the *phyA phyB cry1 cry2* quadruple mutant.

1. Introduction

The light environment fluctuates constantly, thus, the photosynthetic apparatus must operate dynamically. Energy for photosynthesis is harvested by the chloroplast photosystems. In addition, outside the chloroplast, the photoreceptors sense light availability, quality and direction. In Arabidopsis red, far-red light absorbing phytochromes (phys) (*PHYA-PHYE*) (Quail et al., 1995) and UV-A/blue light absorbing cryptochromes (crys) (*CRY1* and *CRY2*) (Cashmore et al., 1999) are among the most important photoreceptors.

Germinating seedlings deetiolate in response to light through coordinated changes in stem and leaf morphology as well as the acquisition of the biochemistry needed for photosynthesis establishment. Phys and crys are the most important photoreceptors that modulate growth and development and thus determine its survival (Mazzella et al., 2001; Strasser et al., 2010). *phyA phyB phyC phyD phyE* quintuple mutants grown under red light develop pale leaves (Strasser et al., 2010), whereas these mutants grown under

Abbreviations: Ci, intercellular CO_2 concentration; Chla, chlorophylla; Chlb, chlorophyll b; cry, cryptochrome; FC, fold change; GO, gene ontology; MS, mass spectrometry; phy, phytochrome; RuBP, ribulose-1,5-biphosphate; 2D, two dimensional gel electrophoresis.

* Corresponding author at: INGEBI Vuelta de Obligado 2490, Buenos Aires 1428, Argentina. Fax: +54 11 4786 8578.
E-mail addresses: mazzella@dna.uba.ar, mazzellaagus@gmail.com (M.A. Mazzella).
[1] Present address: Instituto de Genética Ewald A. Favret, Centro de Investigación en Ciencias Veterinarias y Agronómicas (CICVyA), Instituto Nacional de Tecnología Agropecuaria (INTA), Castelar, Argentina.

http://dx.doi.org/10.1016/j.jplph.2015.07.004
0176-1617/

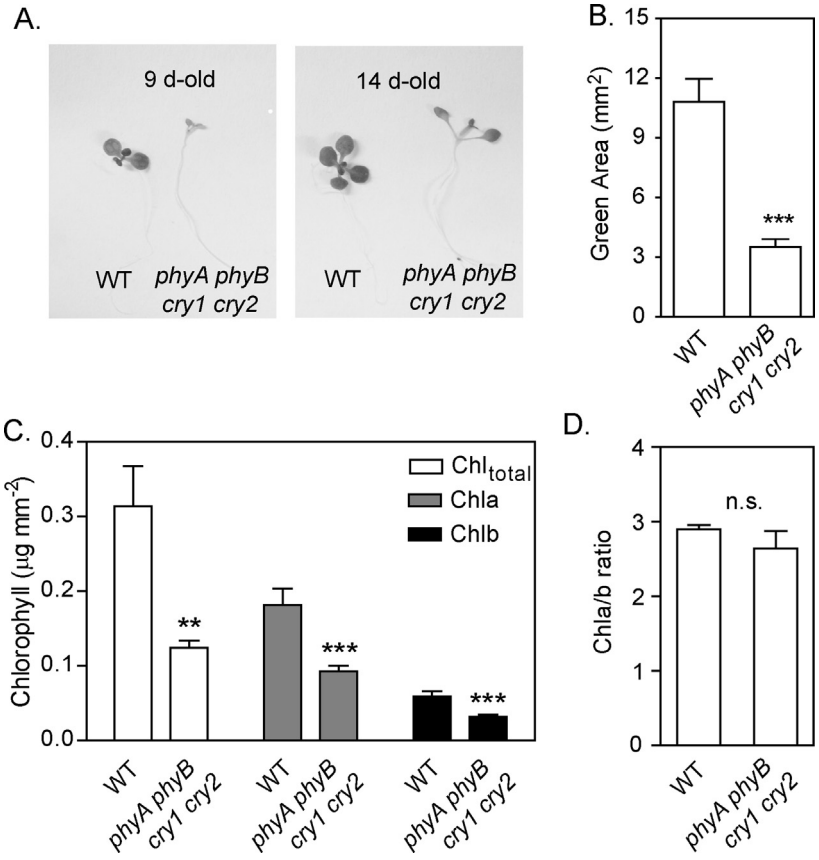

Fig. 1. *phyA phyB cry1 cry2* quadruple mutant phenotype. (A) WT and *phyA phyB cry1 cry2* quadruple mutants were grown under white light on agar plates. WT seedlings were harvested after 9 d, and *phyA phyB cry1 cry2* quadruple mutants were harvested after 14 d (developmental stage 1.02 according to Boyes et al. (2001). (B) Total green area at stage 1.02. (C) Total chlorophyll, chlorophyll a and b contents per unit area at stage 1.02. (D) Chla/b ratios.

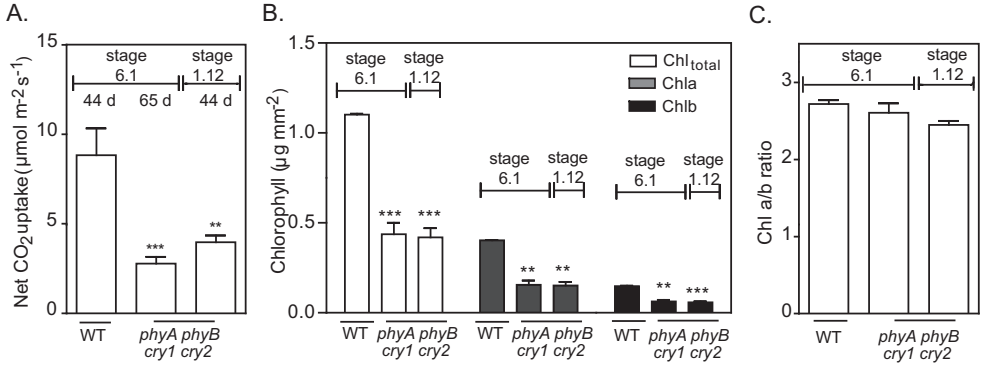

Fig. 2. Net CO_2 uptake is severely affected in the *phyA phyB cry1 cry2* quadruple mutant. (A) Net CO_2 uptake in WT plants grown for 44 d (developmental stage 6.1) under white light and the *phyA phyB cry1 cry2* quadruple mutant grown for 65 d (developmental stage: 6.1) or 44 d (developmental stage 1.12). (B) Total chlorophyll, chlorophyll a and b contents per unit area. (C) Chla/b ratios.

white light develop green leaves. This difference highlights the contribution of cryptochromes during photoautotrophic development (Strasser et al., 2010). When plants lack phyA, phyB, cry1 and cry2, deetiolation and the beginning stages of seedling development are severely affected (Mazzella et al., 2001). The *phyA phyB cry1 cry2* quadruple mutant grown under white light or sunlight conditions displays an etiolated phenotype, the plants do not form normal rosettes, the leaves are pale-green, and leaf production is retarded and occurs at a low rate (Mazzella et al., 2001). Additionally, the transition from the vegetative to the reproductive stage in the *phyA phyB cry1 cry2* quadruple mutant occurs early developmentally but very late in chronologically (Mazzella and Casal, 2001). This altered growth and development of the quadruple mutant could be the consequence of a reduced photosynthetic capacity. Although photosynthesis is reduced in the *phyB* simple and *cry1 cry2* double mutants (Boccalandro et al., 2009, 2012), detailed information about the processes that might affect them have not been described.

In addition to retrograde signaling (the informational signal that flows from the chloroplast to the nucleus), light-dependent synthesis of chlorophyll and proteins during the early developmental stage of chloroplasts can be triggered by photoreceptor-dependent signaling. Signals related to "biogenic control" are those that

affect nuclear transcription during plastid development (Pogson et al., 2008). However, light intensity signals are involved in regulating the function of the photosynthetic apparatus in mature plants; these responses are referred as "operational control" (Pogson et al., 2008; Pogson and Albrecht, 2011). In this regard, approximately 20% of the genes expressed in plant leaves are directly or indirectly regulated by light, most of which are photosynthesis-related nuclear genes (Ruckle et al., 2012). The expression of these genes is reduced when chloroplast function is defective and chloroplast signals are deficient (Pogson et al., 2008). Additionally to control gene transcription, light affects the level of some proteins post-translationally. Upon exposure to light, phys and crys signaling pathways converge on the deactivation of COP1 (Constitutive Photomorphogenic 1) (Lau and Deng, 2012), a photomorphogenic repressor that ubiquitinates and targets positive photomorphogenic transcription factors to be degraded by the 26S proteosome pathway (Osterlund et al., 2000; Holm et al., 2002; Seo et al., 2003; Jang et al., 2005). In addition, protein phosphorylation status changes with a meaningful functional impact during photomorphogenesis (Budde and Randall, 1990; Shen, et al., 2008; Bigeard et al., 2014). In this context, systemic proteome approaches are then necessary to investigate the correlation between transcripts and protein levels.

Two-dimensional gel electrophoresis (2D) has been used to compare protein expression patterns between seedlings grown in dark, red, far-red and blue light (Kim et al., 2006). Protein profiles have also been investigated in *cry1*, *cry1 cry2* and *phyA phyB* mutants in Arabidopsis (Phee et al., 2007; Yang et al., 2008; Xu et al., 2009) and cry2 overexpressors in tomato (Lopez et al., 2012). These studies show that light perception through photoreceptors primarily altered photosynthetic and metabolic proteins.

Because of its role in photosynthesis and morphogenesis, light is the environmental factor that most affects plant architecture. However, there is little information about the protein identity of the photosynthetic-related proteins affected by both families of photoreceptors in a whole proteomic study. In this work, we characterized photosynthetic ability in *phyA phyB cry1 cry2* quadruple mutants and use 2D techniques to detect differences in the proteome between WT and *phyA phyB cry1 cry2* quadruple mutants that could account for their lower photosynthetic capacity.

2. Materials and methods

2.1. Plant material and growth conditions

Seeds of WT *Arabidopsis thaliana* and the *phyA phyB cry1 cry2* quadruple mutant (Mazzella et al., 2001) were in the *Landsberg erecta* background. Seeds were surface sterilized (4 h of exposure to the fumes produced by 1.25% *v*/*v* HCl/NaClO) and sown on 0.8% *w*/*v* agar plates containing one-half-strength Murashige and Skoog basal medium pH 5.7. After 3 d at 4 °C in darkness, the seeds were exposed to a white-light pulse for 2 h to promote germination and then were returned to darkness. When indicated, the seedlings were transferred to specific light conditions at 22°C, 24 h after the light pulse.

For soil-based analysis, 5-day-old seedlings were transplanted to individual pots filled with a mixture of soil:vermiculite:perlite:peat moss (1:1:1:1). The plants were exposed to continual light at 22 °C. The plants were observed daily, and developmental stages were determined following the scale proposed by Boyes et al. (2001).

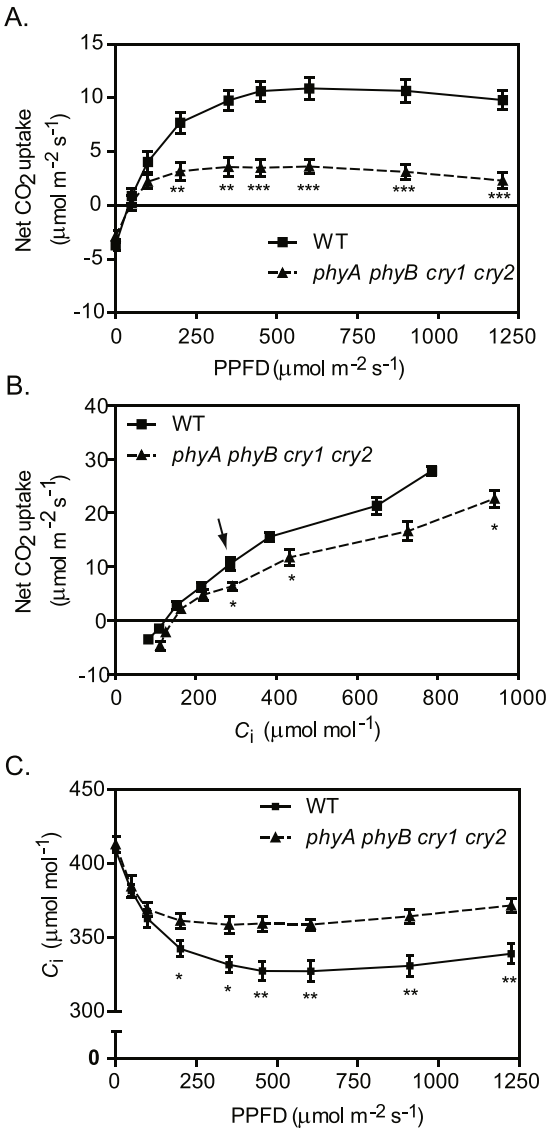

Fig. 3. Light and CO_2 response curves of net CO_2 uptake in WT and *phyA phyB cry1 cry2* quadruple mutant plants. (A) Photosynthetic light response curves at 400 μmol mol^{-1} CO_2. (B) Photosynthetic internal CO_2 response curve at PPFD 900 μmol m^{-2} s^{-1}. (C) Intercellular CO_2 concentration as function of light. Data are the means and se of at least 6 plant replicates. The asterisks denote significant differences (*P < 0.05, **P < 0.005, ***P < 0.001) with the WT according to ANOVA and Bonferroni post tests. The tests were performed on WT and phyA *phyB* cry1 cry2 quadruple mutants having the closest C_i (Note that in every case this underestimates the significance of the difference for the samples). The arrow indicates the C_i that coincides with the ambient CO_2.

2.2. Green area determination and chlorophyll content analysis

The seedlings were photographed, and green areas were calculated using ImageJ Software (Abramoff et al., 2004). Chlorophyll content was determined as described in Arnon (1949).

2.3. Leaf photosynthesis

Leaf CO_2 exchange was measured using a Li-6400 Portable Photosynthesis System (Li-Cor, Lincoln, NE, USA) under 900 photons μmol m^{-2} s^{-1} PPFD (photosynthesis photon flux density). Saturating light was provided by a 6400-40 leaf chamber using a mix of 80% red and 20% blue light. Air flow and CO_2 concentration in the reference chamber were controlled automatically by the equipment at 300 μmol s^{-1} and 400 μmol mol^{-1},

respectively. Green areas were calculated using ImageJ software (Abramoff et al., 2004). Dose response to light was determined at 400 μmol mol^{-1} of CO_2, with the following PPFD sequence: 0, 50, 100, 200, 350, 450, 600, 900, 1200 μmol m^{-2} s^{-1}. Dose response to CO_2 levels was determined with the following sequence of CO_2 concentrations at the reference cell: 400, 300, 200, 100, 50, 400, 600, 1,000, and 1,500 μmol mol^{-1}, setting PPFD at 900 photons μmol m^{-2} s^{-1}.

2.4. Protein extraction protocol and Western blot

Seedlings were ground in liquid nitrogen with mortar and pestle into a fine powder. Light-grown seedlings were harvested at developmental stage 1.02, and proteins were extracted using the phenol extraction protocol (Isaacson et al., 2006). Dark-grown seedlings were harvested 5 d after germination, and proteins were extracted by trichloroacetic acid (TCA) precipitation (Isaacson et al., 2006). Proteins were resuspended in isoelectric focusing (IEF) buffer (7 M urea, 2 M thiourea, 4% *w*/*v* CHAPS) and were centrifuged at 16,000 g for 5 min to remove undissolved content. Protein concentration was determined using Bradford's method (Bradford, 1976). For Western blot experiments, total proteins were extracted from both genotypes at developmental stage 1.02 as indicated above for light-grown plants. For details on the Western blot procedure, see supplementary M&M.

2.5. Two-dimensional polyacrylamide gel electrophoresis (2D PAGE).

The protein samples were separated in the first dimension on the basis of the protein net charge by IEF and in the second dimension on the basis of the protein molecular mass. The samples were prepared for IEF as follows: 200 μg of protein was adjusted to 60 mM DTT, 0.5% *w*/*v* ampholyte pH 3–10 and 0.01% *w*/*v* bromophenol blue (BPB) in 125 μL of IEF buffer for the 7 cm pH 3–10 immobilized pH gradient (IPG) strips; 200 μg of protein was adjusted to 10 mM DTT, 0.5% *w*/*v* ampholyte pH 4–7, 1.2% *v*/*v* DeStreak Reagent (GE Healthcare, USA) and 0.01% *w*/*v* BPB in 125 μL of IEF buffer for the 7 cm pH 4–7 IPG strips; and 450 μg of protein was adjusted to 10 mM DTT, 0.5% *w*/*v* ampholyte pH 4–7, 1.2% *v*/*v* DeStreak Reagent and 0.01% *w*/*v* BPB in 250 μL of IEF buffer for the 13 cm pH 4–7 IPG strips.

The samples were loaded on IPG strips by passive rehydratation for 12 h at 30 °C according to the manufacturer's instructions (GE Healthcare, USA). IEF was carried out using the Ettan IPGphor 3 system (Amersham Biosciences, USA). The 7 cm or 13 cm IPG strip focusing was performed until an accumulated voltage of 8,000 or 19,800 V, respectively. Then, the strips were equilibrated in equilibration buffer (EqB) (50 mM Tris–HCl pH 8.8, 6 M Urea, 30% *v*/*v* glycerol, 2% *w*/*v* SDS, 0.01% *w*/*v* BPB) supplemented with 10 mg/mL DTT for 15 min and with Iodoacetamide for another 15 min. The second dimension was performed on 10% SDS-PAGE for pH 3–10 IPG strips and on 12% SDS-PAGE for pH 4–7 IPG strips. Proteins were visualized by Coomassie brilliant blue G-250 staining, and gel images were acquired using an Image Scanner III (GE Healthcare, USA).

2.6 Image analysis and statistical analysis

Image analysis was performed with ImageMaster 2D Platinum 7.0 Software (Amersham Biosciences, USA). The abundance of each protein spot was estimated by the percentage volume (%Vol). The %Vol remains relatively independent of variations due to protein loading and staining. The %Vol was calculated as follows: $(Vol_{spot}/Vol_{tot}) \times 100$, where Vol_{spot} is the volume above the spot outline, which is situated at 75% of the spot height (Fig. S1), and Vol_{tot} is the sum of all of the Vol_{spot}. The %Vol was used as an input list for the statistical analysis carried out using the package Limma (Smyth, 2005) in the R computing environment. Spots matched in at least 3 of the 4 WT gels, and 3 of the 4 *phyA phyB cry1 cry2* quadruple mutant gels were selected for the analysis. %Vol was transformed to Log (%Vol). Two inter-gels normalization methods were examined: Scale and Quantile (Fig S1). These methods were developed for the normalization of array data and are useful for the normalization of proteomic data (Kultima et al., 2006). An optimal normalization was obtained applying the Quantile algorithm (for further information, see Fig S1). Normalized data were fitted to the lmFit Limma function (Smyth, 2005). Moderated t-statistics were computed by the empirical Bayes method (Smyth, 2004). The spots with a *P*-value < 0.05 and fold change >1.5 were considered to be differentially expressed. The spots clearly observed as unique peaks were excluded. The gel pieces were processed in the mass spectrometry (MS) facility CEQUIBIEM in Argentina (for further information, see Supplementary Materials and methods).

Web-based data analyses are detailed in Supplementary Materials and methods.

3. Results

3.1. Delayed development of the phyA phyB cry1 cry2 quadruple mutant

In the *phyA phyB cry1 cry2* quadruple mutant compared to the WT, leaf appearance and the transition to the flowering stage are delayed, whereas life span is extended, both in long-day and continuous light conditions (Mazzella et al., 2001). To discriminate changes in physiology and protein abundance that are due to the lack of the four photoreceptors, we compared WT and *phyA phyB cry1 cry2* quadruple mutant plants at the same developmental stage, rather than similar chronological development. We followed the developmental scale proposed by Boyes et al. (2001).

At developmental stage 1.02, the seedlings have the first cotyledon fully opened and the first pair of visible leaves longer than 1 mm. This stage was reached at 9 d in WT seedlings but at 14 d in the *phyA phyB cry1 cry2* quadruple mutant; note that after 9 d, the light-grown quadruple mutant does not even display its first pair of leaves (Fig. 1A). At stage 1.02, the green area of the quadruple mutants was 3.5 times smaller than that of the WT. It also showed 3 times less total chlorophyll content per unit area and less chlorophyll a (Chla) and chlorophyll b (Chlb) when compared to WT (Fig. 1C). However, no differences were observed in the Chla/b ratio (Fig. 1D).

3.2. Photosynthesis is severely affected in the phyA phyB cry1 cry2 quadruple mutant

The life span extension and the described phenotypes of the *phyA phyB cry1 cry2* quadruple mutant described above may be linked to an energetic deficiency (Minina et al., 2013; Lastdrager et al., 2014). Thus, we measured net CO_2 interchange in fully developing leaves in stage 6.1 plants, corresponding to a midflowering stage reached after 44 d in the WT and 65 d in the quadruple mutant. Because the *phyA phyB cry1 cry2* quadruple mutant displayed senescent leaves after 65 d, we also studied mutant plants in stage 1.12 (44 d) that showed fully green leaves. Compared to the WT, the *phyA phyB cry1 cry2* quadruple mutant showed significantly reduced (65–70%) net CO_2 uptake (Fig. 2A) and reduced total chlorophyll content per unit area (Fig. 2B) at both developmental stages. Again, Chla and Chlb were reduced in the quadruple mutant, while the Chla/b ratio remained unaffected (Fig. 2B, C)

To further define the photosynthetic characteristics of the quadruple mutant, we studied the photosynthetic response to irradiance and to intracellular CO_2 concentration. We found that

net CO_2 exchange in darkness was unaffected by the *phyA phyB cry1 cry2* mutation, suggesting that there were no differences in mitochondrial respiration rates (Fig. 3A). The quantum efficiency, estimated by the slope along the linear portion at low PPFD, was similar for both genotypes (Fig. 3A). The light saturation point was 450 $\mu mol\ m^{-2}\ s^{-1}$ for WT plants and was significantly lower for the quadruple mutant (200 $\mu mol\ m^{-2}\ s^{-1}$) (Fig. 3A). The maximum rate for CO_2 fixation (P_{max}) was significantly reduced in the quadruple mutant (WT: 10.9 ± 1.0; quadruple mutant: 3.6 ± 0.7, $P < 0.001$), suggesting a severe reduction in photosynthetic ability (approximately 66%) at high irradiances.

Fig. 3B shows that net CO_2 uptake increased with intracellular CO_2 levels in both WT and quadruple mutant plants. The net CO_2 uptake is Rubisco-limited at low C_i, whereas it is RuBP-regeneration-limited at high C_i. To define the point that discriminates between low and high CO_2 internal concentration (C_i), we chose the C_i value that corresponded to the external CO_2 concentration (370 $\mu mol\ mol^{-1}$). This point was the fifth value of the curve (C_i 280 $\mu mol\ mol^{-1}$; see arrow in Fig. 3B) that was measured at 400 $\mu mol\ mol^{-1}$ of external CO_2. At a C_i of 280 $\mu mol\ mol^{-1}$, net CO_2 uptake in the quadruple mutant was significantly lower when compared to the WT, suggesting a reduced Rubisco carboxylation efficiency in the quadruple mutant. However, apart from the fifth point, none of the other points showed significant differences at low C_i values. It has been found that there is a transition from both limitation phases approximately 200 and 300 $\mu mol\ mol^{-1}$ (Sharkey et al., 2007). Thus, with the present data, we cannot provide conclusive result about this part of the curve. At a high C_i, the net CO_2 uptake of the quadruple mutant was significantly reduced compared to the WT (Fig. 3B). Fig. S3 showed that the photosynthetic rate on a chlorophyll basis was similar in both WT and quadruple mutant. We hypothesize that this photosynthesis limitation is non-stomatic because the internal concentration of CO_2 was higher in the quadruple mutant than in WT plants (Fig. 3C).

3.3. *Proteome map of the differentially expressed proteins between white light-grown WT and* phyA phyB cry1 cry2 *quadruple mutant seedlings*

To identify the most abundant proteins differentially expressed in the *phyA phyB cry1 cry2* quadruple mutant that would support its less photosynthetic phenotype, we performed 2D-gels of total proteins extracted from WT and *phyA phyB cry1 cry2* quadruple mutant light-grown seedlings at developmental stage 1.02. When total proteins were resolved using a strip with a pH range of 3–10 (7 cm) followed by standard SDS-PAGE (Fig. 4A, B), 36 out of 194 spots (18.5% of the total number of spots) were significantly different between the WT and the quadruple mutant. Eleven under-expressed spots and four over-expressed spots in the quadruple mutant compared to the WT were identified by MS (Fig. 4A, B; Table 1).

To improve spot resolution and detection, we used strips with pH ranges of 4–7 and 13 cm large. From 354 spots that were matched between gels, 62 (17.5%) spots showed significant differences ($P < 0.05$), with 34 under-expressed and 28 over-expressed in the *phyA phyB cry1 cry2* quadruple mutant compared to the WT. From these, we identified 15 under-expressed spots (representing 12 unique proteins) and 15 over-expressed spots (representing 13 unique proteins) (Fig. 4C, D; Table 1). The spot number 75 represented two different proteins and was not included in later analyses.

Three under-expressed proteins (FRN2, PSBO-2 and RCA) and four over-expressed proteins (FDH, PATL2, COR47 and PcaP1) were independently identified in both gels (Table 1), reinforcing the reproducibility and robustness of the analysis. PATL2 expression was determined to be down-regulated (spot 670: MW 102.8 *pI*: 5.65) but also up-regulated (spot 991: MW 149.7 *pI* 5.08) (Table 1 and Fig. 4C, D). The difference in the *pI* between both spots could be the result of photoreceptor-dependent phosphorylation. Additionally, other proteins that might have different isoforms include FNR2 (spots 292 and 24), PSBO-2 (spots 10 and 9), FNR1 (spots 25 and 290) and PYK10-binding protein (spots 389 and 28) (Table 1).

To analyse whether the changes in protein expression were due to light exposure instead of genetic background, we ran total proteins extracted from 5-day-old dark-gown WT and quadruple mutant seedlings. After 5 d in complete darkness, both genotypes were phenotypically indistinguishable, suggesting that the proteome changes found in light-grown quadruple mutants were due to light exposure and not to genetic background. Only four spots over-expressed in quadruple mutants, representing 2 proteins: 12 S storage protein CRA1 and CRUCIFERIN 3 (Fig. S4). These results are consistent with the increased expression of the *CRA1* and *CRU3* transcript levels reported for dark-grown *phyB* mutant seedlings (Mazzella et al., 2005).

3.4. *Functional classification of the proteins affected in* phyA phyB cry1 cry2 *quadruple mutants*

The under-expressed proteins in the *phyA phyB cry1 cry2* quadruple mutant fell into nine Gene Ontology (GO) enriched categories: photosynthesis, generation of metabolic and energy precursors, catabolic processes, biosynthesis processes, carbohydrate metabolism, response to a biotic stimulus, response to an abiotic stimulus, response to stress and cellular organization components (Table 2). Specifically, 9 proteins are localized to chloroplast and are directly involved in photosynthesis: PRK, GAPB, RCA and FAB5 are involved in the Calvin cycle, whereas PSBO2, FNR1, FNR2, ATPA and ATPC are involved in energy metabolism, as they are part of the photosynthesis light reaction center (Fig. S5A). The central spot corresponding to the large subunit of the Rubisco was not included in the analysis because that spot was not well focused due to its high concentration (Fig S6). As Rubisco is a limiting factor in photosynthesis rates and the curve response at low CO_2 was not conclusive (Fig. 3B), we quantified its expression level by western blot (Fig 5). The Rubisco L was 3 times less expressed in the *phyA phyB cry1 cry2* quadruple mutant compared to the WT (Fig 5).

Other under-expressed proteins identified in the *phyA phyB cry1 cry2* quadruple mutant were associated with chloroplast function: AtSCO1 and CSP41B are involved in chloroplast organization; VAR2 participates in thylakoid membrane biogenesis; CSP41A has ribonuclease activity involved in plastid rRNA maturation; and the protein identified as At2g37660 is a copper ion binding protein. The rest of the under-expressed proteins corresponded to mitochondrial and peroxisomal proteins involved in photorespiration, such as AGT1, SHM1 and GGT1 (Fig. S5A, Table 2). The Biological GO terms enriched among the over-expressed proteins in the quadruple mutant belonged to the “response to stress” or “response to abiotic stimuli” categories (Table 2).

Fourteen of the 20 under-expressed proteins identified in the quadruple mutant localized within the chloroplast, according to the chloroplastic data base published by Ferro et al. (2010). Eight localized to the stroma (RCA; AT2G37660, GAPB, PRK, SCO1, FAB5, CSP41A and CSP41B) and 6 to the thylakoid (VAR2, FRN1, FNR2, ATPC1, ATPA, PSBO-2). However, the over-expressed proteins did not show a significant specific subcellular localization, and none of them were found in the chloroplast proteome (Ferro et al., 2010). A thorough analysis of the under-expressed proteins under the GO term “cellular organization” generated two subcategories: ‘chloroplast organization’ and ‘thylakoid membrane organization’ (Table 2).

Table 1
Identification and characterization of under- and over-expressed spots in the *phyA phyB cry1 cry2* quadruple mutants.

Down-regulated spots in the *phyA phyB cry1 cry2* quadruple mutant															
pH 3–10					pH 4–7										
Spot[a]	Exp (MW/pI)[b]	*Mat-ches*[c]	SC (%)[d]	Score[e]	Spot[a]	Exp (MW/pI)[b]	*Mat-ches*[c]	SC (%)[d]	Score[e]	Theo. MW/pI[f]	AGI[g]	Protein name	Cellular process[h]	FC[i] 3–10	FC[i] 4–7
67	38.3/7.02	14	44	194						42.6/8.41	AT1G09340	Chloroplast stem-loop binding protein of 41 kDa (CSP41B)	RNA. Transcriptional regulation.	2.0	
83	40.9/5.34	12	46	288						44.0/5.91	AT1G32060	Phosphoribulokinase (PRK)	PS. Calvin cycle.	1.7	
90	42.4/8.3	13	50	344						44.2/7.95	AT2G13360	Alanine:Glyoxylate aminotransferase (AGT)	PS. Peroxisomal aminotransferase.	1.6	
96	42.7/6.33	5	8	97						43.0/6.78	AT1G42970	Glyceraldehyde-3-phosphate dehydrogenase b subunit (GAPB)	PS. Calvin cycle.	1.5	
114	49.3/6.78	16	36	367						53.3/6.88	AT1G23310	Glutamate:Glyoxylate aminotransferase 1 (GGT1)	PS. Peroxisomal aminotransferase.	1.6	
167	79.3/5.25	21	39	429						86.1/5.28	AT1G62750	Snowy cotyledon1 (SCO1)	Protein synthesis. Elongation.	1.7	
178	97/5.96	7	7	103						114/6.63	AT2G26080	Glycine decarboxylase p-protein 2 (GLDP2)	PS. Photorespiration/ C1 Metabolism.	2.0	
226	52.8/7.4	20	38	229						57.0/8.37	AT4G37930	Serine hydroxymethyltransferase 1 (SHM1)	C1 Metabolism.	1.6	
18	28.9/5.13	23	70	473	9	28/5.05	8	34	315	35.0/5.96	AT3G50820	Photosystem II subunit O-2 (PSBO-2)	PS. Light reaction.	1.7	1.8
					10	27.7/5.15	11	44	363						1.8
50	33.7/6.76	11	29	218	24	32.5/6.37	17	53	256	28.0/8.51	AT1G20020	Ferredoxin-NADP(+)-oxidoreductase 2 (FNR2)	PS. Light reaction.	1.6	1.9
					292	32.8/6.63	17	46	410						1.7
105	45.3/5.1	13	45	411	96	44.5/5.06	8	25	231	52.0/5.93	AT2G39730	Rubisco activase (RCA)	PS. Calvin cycle.	1.5	1.7
					25	32.5/5.86	16	56	388	40.3/8.3	AT5G66190	Ferredoxin-NADP(+)-Oxidorreductase 1 (FNR1)	PS. Light reaction.	1.9	
					290	32.4/5.69	15	43	433					1.6	
					26	34.2/5.90	7	25	137	32.9/5.80	AT2G38230	Pyridoxine biosynthesis (PDX)	Cofactor, vitamins metabolism.	2.9	
					44	37.2/6.52	5	9	246	43.9/8.74	AT3G63140	Chloroplast stem-loop binding protein of 41 kDa (CSP41A)	RNA. Transcriptional regulation.	1.7	
					71	40.5/5.87	6	25	313	38.3/5.53	AT4G26530	Fructose-bisphosphate aldolase 5 (FBA5, M3E9.40)	PS. Calvin cycle. Glycolysis.	2.0	
					169	55.3/5.28	16	31	304	55.3/4.9	ATCG00120	ATP synthase subunit alpha (ATPA)	Metabolism. PS.	1.8	
					194	62.2/5.32	11	32	237	74.2/6.24	AT2G30950	*Variegated* 2 (VAR2)	Regulation. Protein degradation. Metalloprotease.	1.7	

Table 1 (*Continued*).

Down-regulated spots in the *phyA phyB cry1 cry2* quadruple mutant

pH 3–10					pH 4–7									
Spot[a]	Exp (MW/pI)[b]	*Mat-ches*[c]	SC (%)[d]	Score[e]	Spot[a]	Exp (MW/pI)[b]	*Mat-ches*[c]	SC (%)[d]	Score[e]	Theo. MW/pI[f]	AGI[g]	Protein name	Cellular process[h]	FC[i] 3–10	FC[i] 4–7
					297	37.2/6.28	13	43	228	40.9/8.17	AT4G04640	Gamma subunit of chloroplast ATP synthase (ATPC1)	PS. Light reaction.	1.9	
					670	102.8/5.64	7	15	99	60/4.59	AT1G22530	*Patellin 2* (PATL2)	Transport.		1.8
					995	28.7/5.58	8	38	272	34.9/8.64	AT2G37660	NAD(P)-binding Rossmann-fold superfamily protein (F13M22.16)	Unknown.		1.7

Up-regulated spots in the *phyA phyB cry1 cry2* quadruple mutant

pH 3–10					pH 4–7										
Spot[a]	Exp (MW/pI)[b]	*Mat-ches*[c]	SC%[d]	Score[e]	Spot[a]	Exp (MW/pI)[b]	*Mat-ches*[c]	SC (%)[d]	Score[e]	Theo. (MW/pI)[f]	AGI[g]	Protein name	Cellular process[h]	FC[i] 3–10	FC[i] 4–7
61	37.3/5.02	4	21	219	411	36.0/5.12	3	––	69	24.7/4.65	AT4G20260	Plasma-membrane associated cation-binding protein 1 (PCAP1)	Signaling.	1.7	2.4
94	42/6.70	6	25	97	967	42/6.61	13	49	474	42.4/7.59	AT5G14780	Formate Deshydrogenase (FDH)	C1 Metabolism.	2.1	2.3
187	145.4/4.96	11	28	164	991	149.7/5.08	10	21	189	60/4.59	AT1G22530	Patellin 2 (PATL2)	Transport.	1.5	2.0
234	55/4.39	11	60	233	166	55.3/4.55	9	48	215	29.9/4.44	AT1G20440	Cold regulated protein 47 (COR47)	Abiotic stress	2.3	2.3
					18	30.0/4.89	9	33	283	33.36/4.44	AT1G35160	General regulatory factor 4 (GRF4)	Signaling.		1.6
					28	33.2/5.66	6	27	109	32.2/5.56	AT3G16420	PYK10-binding protein 1 (PBP1)	PYK10 Molecular chaperone		1.9
					389	34/5.52	9	34	284						1.8
					75	41.3/6.00	13 11	34 28	310121		AT2G20420 AT1G01560	ATP citrate lyase (ACL) family protein MAP kinase 11 (MPK11)			
					106	46.2/5.81	16	53	389	42.8/5.60	AT3G17390	Methionine adenosyltransferase 4 (MTO3)	Metals union protein		
					131	50.8/4.73	13	40	305	43.5/4.42	AT5G39570	MIJ24.6. NM_123319	Unknown.		
					181	58.7/4.92	8	19	69	56.4/4.64	AT1G77510	Protein disulfide isomerase 6 (PDI6)	Redox.	1.7	
					953	37.2/5.37	20	69	328	36.2/5.02	AT1G35720	Annexin 1 (ANNAT1)	Cell organization.	1.9	
					966	38.0/4.80	6	45	211	20.8/5.2	AT1G76180	Early response to dehydration 14 (ERD14)	Abiotic stress.		3.2
					989	95.0/5.03	7	10	143	64/4.5	AT1G72150	Patellin 1 (PATL1)	Transport.		1.7

[a] Spot number.
[b] Experimental MW(kDa)/pI.
[c] Number of peptides for which mass/charge match with the picks observed by MS.
[d] Protein sequence coverage.
[e] Score generated by Mascot; protein scores greater than 61 are significant ($P < 0.05$).
[f] Theorical MW (kDa)/pI (TAIR).
[g] Arabidopsis Gene identifier.
[h] Cellular process, information from the PPBD and MapMan, PS: Photosynthesis.
[i] fold change.

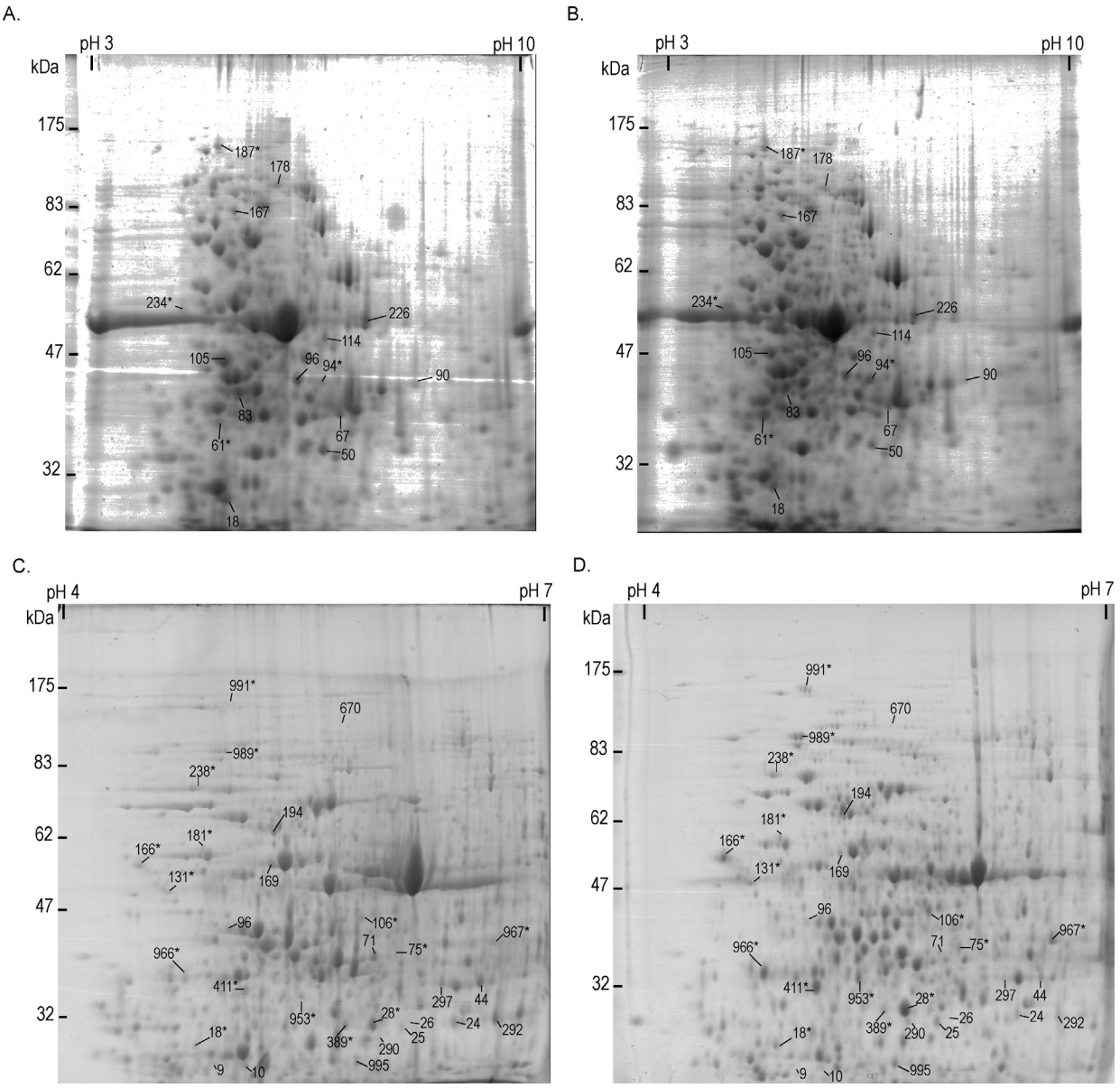

Fig. 4. Representative 2D gel images showing protein expression changes between the white light-grown WT and the *phyA phyB cry1 cry2* quadruple mutant. Proteins were resolved according to their isoelectric point in the first dimension and according to their molecular weight in a second dimension. (A, B) Representative gel images for total proteins resolved in strips with a *pH* range of 3 to 10 and 7 cm from WT (A) or *phyA phyB cry1 cry2* quadruple mutant (B) seedlings. (C, D) Representative gel image for total proteins resolved in strips with a pH range of 4–7 and 13 cm from WT (C) or *phyA phyB cry1 cry2* quadruple mutant (D) seedlings. Statistical analysis of differentially expressed proteins was calculated from four independent replicates of each 2D gel. Spots identified by MS are indicated with the number of the spot. Spot numbers marked with an asterisk indicate over-expressed proteins, while those without asterisk indicate under-expressed proteins in the *phyA phyB cry1 cry2* quadruple mutant compared with the WT.

A network generated on GeneMANIA showed that under-expressed proteins produced a cluster (clustering coefficient 0.937), whereas the over-expressed proteins did not form a closely related group (clustering coefficient 0.580) (Fig. S5B).

Most of the under-expressed proteins in the light-grown *phyA phyB cry1 cry2* quadruple mutant were specifically involved in the Calvin cycle (including Rubisco) or were components of the light reaction center, suggesting that depletion of all of these proteins would have a negative impact on the photoautotrophic ability of quadruple mutants.

4. Discussion

Here, we studied the photosynthetic ability of light-grown seedlings in the absence of the four main photoreceptors (phyA, phyb, cry1 and cry2) in *A. thaliana* and used 2D gel coupled with MS to identify their protein profiles. The autotrophic development of the *phyA phyB cry1 cry2* quadruple mutant was severely affected when grown under white light. The *phyA phyB cry1 cry2* quadruple mutant showed severe reductions in chlorophyll levels per area (60%) (Fig. 1C and Fig. 2B), net photosynthetic CO_2 uptake at high irradiances (66%) (Fig. 2A and Fig. 3A), Rubisco levels (3-fold) (Fig. 5) and the expression of several chloroplast localized proteins that are part of the light reaction centers or are involved in the Calvin Cycle (Tables 1 and 2; and Fig. S5A). Under similar conditions, the *phyB* single and *cry1 cry2* double mutants displayed a reduction in the photosynthetic rates at high irradiances of approximately 35% compared to the WT (Boccalandro et al., 2009, 2012). All of these results suggest that redundancy between phys and crys might regulate the photosynthesis process at high irradiances.

Table 2
Gene ontology term enrichment of the up- and down-regulated proteins in the quadruple mutant *phyA phyB cry1 cry2*.

Down regulated in the *phyA phyB cry1 cry2* quadruple mutant

1. Slim GO — biological process

GO	Description	Adjusted *p*-value	Group frequency	Genome frequency	Protein name
15979	Photosynthesis	1.65E-20	14/20 70.0%	419/30507 1.3%	SCO1CSP41A RCA GAPB PRK FNR1 ATPC1 SHM1 FNR2 ATPA VAR2 PSBO-2CSP41B AT2G37660
6091	Generation of precursor metabolites and energy	4.09E-20	15/20 75.0%	664/30507 2.2%	SCO1CSP41A RCA GAPB PRK FNR1 ATPC1 SHM1 FNR2 ATPA VAR2 PSBO-2CSP41B AT2G37660 FAB5
9056	Catabolic process	2.25E-13	16/20 80.0%	2530/30507 8.2%	SCO1CSP41A GAPB PRK FNR1 GGT1 ATPC1 SHM1 FNR2 ATPA VAR2 PSBO-2CSP41B GLDP2 AT2G37660 FAB5
9058	Biosynthetic process	8.97E-11	18/20 90.0%	5639/30507 18.4%	SCO1CSP41A RCA PDX AGT GAPB PRK FNR1 GGT1 ATPC1 FNR2 SHM1 ATPA VAR2 PSBO-2CSP41B AT2G37660 FAB5
5975	Carbohydrate metabolic process	1.31E-10	13/20 65.0%	1941/30507 6.3%	SCO1CSP41A GAPB PRK FNR1 ATPC1 FNR2 ATPA VAR2CSP41B PSBO-2 AT2G37660 FAB5
9628	Response to abiotic stimulus	4.47E-10	14/20 70.0%	2755/30507 9.0%	CSP41A RCA AGT GAPB PRK FNR1 GGT1 SHM1 FNR2 ATPA VAR2 PSBO-2CSP41B AT2G37660
9607	Response to biotic stimulus	7.07E-08	10/20 50.0%	1533/30507 5.0%	FNR1 PRK FNR2 SHM1 ATPA RCA PSBO-2CSP41B GAPB AT2G37660
6950	Response to stress	6.73E-07	13/20 65.0%	4075/30507 13.3%	RCA AGT GAPB PRK FNR1 GGT1 SHM1 FNR2 ATPA VAR2CSP41B PSBO-2 AT2G37660
16043	Cellular component organization	7.63E-06	11/20 55.0%	3337/30507 10.9%	FNR1 PRK SCO1 ATPC1CSP41A FNR2 VAR2 PSBO-2CSP41B GAPB AT2G37660

2. Biological process enriched inside "Cellular component organization"

9658	Chloroplast organization	8.33 E-8	6/20 30.0%	250/28699 0.8%	PRK SCO1 VAR2 PSBO-2CSP41B GAPB
10027	Thylakoid membrane organization	2.80 E-5	4/20 20.0%	198/28699 0.6%	SCO1 VAR2 PSBO-2CSP41B

Up-regulated in the *phyA phyB cry1 cry2* quadruple mutant

3. Slim GO — biological process

GO	Description	Adjusted *p*-value	Group frequency	Genome frequency	Protein name
6950	Response to stress	3.50 E-04	8/12 66.6%	4075/30507 13.3%	MTO3 PCAP1 PATL1COR47 PDI6 ERD14 FDH ANNAT1
9628	Response to abiotic stimulus	3.50 E-04	7/12 58.3%	2755/30507 9.0%	MTO3 PCAP1 PATL1COR47 PDI6 ERD14 ANNAT1

Total chlorophyll levels were reduced in the quadruple mutant, but the quantum yields were not different (Figs. 2 and 3). This suggests that at very low light levels, the quadruple mutant conserved enough chlorophyll and light harvesting complex proteins to harvest all of the available photons. The fact that the Chla/b ratios did not change in the quadruple mutant suggests that both types of photosystems were reduced to the same level. *phyA* and *phyB* single mutants have reduced total chlorophyll levels relative to the WT, but the Chla/b ratio did not change when the plants were grown under white light (Brouwer et al., 2014). Additionally, in shaded grown plants, total chlorophyll content was decreased, but the Chla/b ratios were unaffected (Murchie and Horton, 1997; Zivcak et al., 2014). Although the abundance of light harvesting complex proteins (LHCs) is directly related to Chlb levels and is transcriptionally activated by phyA, phyB, cry1 and cry2 (Cerdán et al., 1997; Mazzella et al., 2001), we did not identify downregulated LHC proteins in the quadruple mutant. This would most likely be associated with a failure in the identification by MS or fold changes between genotypes less than 1.5 not being considered despite potential significant differences. As evidence that LHC proteins should be down-regulated in the quadruple mutant, we identified some of them as part of the interactome core with a high level of confidence (Fig. S5B).

At high irradiance, the photosynthesis rate was severely reduced in the quadruple mutant (Fig. 3A). This result suggests that this might be the result of the reduction in electron transport and photosynthetic biochemical processes. Several studies showed Rubisco limitation in *phyA phyB cry1 cry2* quadruple mutants. First, Rubisco expression levels were reduced by threefold in the quadruple mutant (Fig 5). Second, the expression of Rubisco activase, the only enzyme that activates Rubisco, is also reduced in the quadruple mutant (Table 1). Third, the light saturation point is lower in the quadruple mutant (Fig. 3A). Fourth, C_i was higher in the quadruple mutant (Fig. 3C). When Rubisco capacity limits photosynthesis, the initial slope of the CO_2 response curve is reduced. Even if we could not arrive to a conclusive result from our data, the net CO_2 exchange of *phyB* and *cry1 cry2* mutants were reduced at low C_i (Boccalandro et al., 2009, 2012). All of these suggest that Rubisco might be a limiting factor of photosynthesis in the quadruple mutant.

At elevated C_i levels, the net CO_2 exchange was significantly reduced in the quadruple mutant, suggesting a limitation on ribulose-1,5- biphosphate (RuBP) regeneration. The RuBP

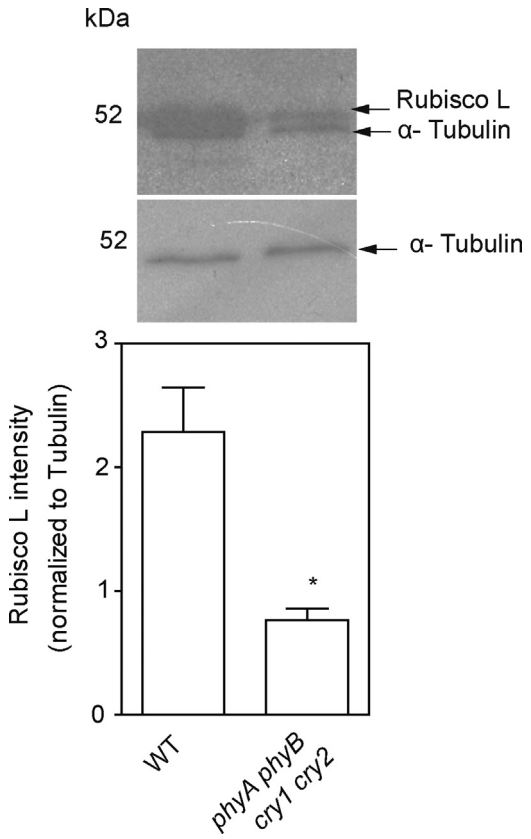

Fig. 5. Rubisco L is under-expressed in the *phyA phyB cry1 cry2* quadruple mutant. Representative Western blot of total protein extracts of WT and *phyA phyB cry1 cry2* quadruple mutant seedlings in stage 1.02 probed first with anti- α Tubulin antibody (middle panel) and then with anti-Rubisco L antibody (top panel). Antibody intensity signals were quantified using ImageJ software. Rubisco L plus Tubulin were normalized against Tubulin for each protein sample (bottom panel, WT $n = 3$, *phyA phyB cry1 cry2* $n = 2$, $^{*}P < 0.05$).

regeneration rate is determined by either the electron transport capacity to generate NADPH and ATP or the activity of the Calvin cycle. Our results supported this observation. First, the severe reduction in P_{max} in the quadruple mutant suggests a reduced activity of the Calvin cycle and electron transport components. Second, MS analysis showed that the quadruple mutant displayed reduced expression in several enzymes involved in the Calvin cycle (including Rubisco) and proteins of the light reaction centers (Table 1). Photosynthesis on a per chlorophyll basis was similar to that of the WT (Fig. S3). In the quadruple mutant, there is an overall reduction in the levels of photosynthetic components, such as total chlorophyll, Rubisco, electron transport and enzymes of the Calvin cycle. These results suggest that protein and pigment reduction might occur simultaneously. Despite the loss of four of the most important photoreceptors, it seems that the correct stoichiometry for the assembly of chloroplast components occurs in the quadruple mutant. Further studies would be necessary to support this idea and to study the integration of photoreceptor signaling and the chloroplast signaling to the nucleus.

phyB and *cry1 cry2* mutants displayed reduced stomata opening under specific wavelength lights (Mao et al., 2005; Wang et al., 2010). However, reduced stomata opening appears to be a consequence rather than a cause of reduced photosynthesis in the quadruple mutant. The higher C_i in the quadruple mutant (Fig. 3C) suggests that this accumulation might be responsible for the stomata closure. Thus, the reduced photosynthesis in the quadruple mutant is nonstomatic.

The increased expression level of photosynthetic-related proteins by light is regulated at the transcriptional level by promoting the degradation of the photomorphogenic negative regulator PIFs (phytochrome interacting factors) (Shin et al., 2009) and by promoting the transcription of photosynthetic gene HY5 (elongated hypocotyl 5) (Oyama et al., 1997; Lee et al., 2007). Thus, transcriptional regulation of 17 of the 20 genes corresponding to the under-expressed proteins in the quadruple mutant, were induced in 3 d dark-grown Arabidopsis seedlings exposed for 4 h to red, far-red or blue-light (Peschke and Kretsch, 2011) (Fig. S7). Our proteomic results complement the transcriptomic data that link photoreceptor activity to specific photosynthetic and energy related proteins.

5. Conclusions

In this work, we studied the photosynthetic ability of the *phyA phyB cry1 cry2* quadruple mutant. We also identified the most abundant proteins differently expressed in the light-grown quadruple mutant that might account for its phenotype. The less photosynthetic capacity of the quadruple mutant could be explained as a simultaneous reduction in the levels of key photosynthetic components that ultimately limit RuBP regeneration, such as total chlorophyll, Rubisco, enzymes involved in the Calvin Cycle and the electron transport system. At low irradiances, these alterations did not modify either the net CO2 uptake or the quantum efficiencies. However, at high irradiances, these alterations resulted in a severe deficiency in CO_2 uptake, which negatively impacted *phyA phyB cry1 cry2* quadruple mutant growth and development.

Acknowledgements

This work was financially supported by grants from FONCyT, Fondo Nacional de Ciencia y Técnica (PICT 2010 #1821) to M.A.M and PICT 2007 # 01976 to J.P.M.

Appendix A. Supplementary data

Supplementary data associated with this article can be found, in the online version, at http://dx.doi.org/10.1016/j.jplph.2015.07.004

References

Abramoff, M., Magelhaes, P., Ram, S., 2004. Image processing with ImageJ. Biophotonics Int. 11 (7), 36–42.
Arnon, D.I., 1949. Copper enzymes in isolated chloroplasts. Polyphenoloxidase in Beta vulgaris. Plant Physiol. 24 (1), 1–15.
Bigeard, J., Rayapuram, N., Pflieger, D., Hirt, H., 2014. Phosphorylation-dependent regulation of plant chromatin and chromatin-associated proteins. Proteomics 14 (19), 2127–2140.
Boccalandro, H.E., Rugnone, M.L., Moreno, J.E., Ploschuk, E.L., Serna, L., Yanovsky, M.J., Casal, J.J., 2009. Phytochrome B enhances photosynthesis at the expense of water-use efficiency in *Arabidopsis*. Plant Physiol. 150 (2), 1083–1092.
Boccalandro, H.E., Giordano, C.V., Ploschuk, E.L., Piccoli, P.N., Bottini, R., Casal, J.J., 2012. Phototropins but not cryptochromes mediate the blue light-specific promotion of stomatal conductance, while both enhance photosynthesis and transpiration under full sunlight. Plant Physiol. 158 (3), 1475–1484.
Boyes, D.C., Zayed, A.M., Ascenzi, R., McCaskill, A.J., Hoffman, N.E., Davis, K.R., Gorlach, J., 2001. Growth stage-based phenotypic analysis of *Arabidopsis*: a model for high throughput functional genomics in plants. Plant Cell 13 (7), 1499–1510.
Bradford, M.M., 1976. A rapid and sensitive method for the quantitation of microgram quantities of protein utilizing the principle of protein-dye binding. Anal Biochem. 72, 248–254.
Brouwer, B., Gardeström, P., Keech, O., 2014. In response to partial plant shading, the lack of phytochrome A does not directly induce leaf senescence but alters the fine-tuning of chlorophyll biosynthesis. J. Exp. Bot.
Budde, R.J.A., Randall, D.D., 1990. Light as a signal influencing the phosphorylation status of plant proteins. Plant Physiol. 94 (4), 1501–1504.
Cashmore, A.R., Jarillo, J.A., Wu, Y.J., Liu, D., 1999. Cryptochromes blue light receptors for plants and animals. Science 284 (5415), 760–765.

Cerdán, P.D., Staneloni, R.J., Casal, J.J., Sánchez, R.A., 1997. A 146bp fragment of the tobacco Lhcb1*2 promoter confers very-low-fluence: low-fluence and high-irradiance responses of phytochrome to a minimal CaMV 35S promoter. Plant Mol. Biol. 33 (2), 245–255.
Ferro, M., Brugière, S., Salvi, D., Seigneurin-Berny, D., Court, M., Moyet, L., Ramus, C., Miras, S., Mellal, M., Le, G., all, S., Kieffer-Jaquinod, S., Bruley, C., Garin, J., Joyard, J., Masselon, C., Rolland, N., 2010. AT_CHLORO, a comprehensive chloroplast proteome database with subplastidial localization and curated information on envelope proteins. Mol. Cell Proteom. 9 (6), 1063–1084.
Holm, M., Ma, L.G., Qu, L.J., Deng, X.W., 2002. Two interacting bZIP proteins are direct targets of COP1-mediated control of light-dependent gene expression in *Arabidopsis*. Genes Dev. 16 (10), 1247–1259.
Isaacson, T., Damasceno, C.M., Saravanan, R.S., He, Y., Catala, C., Saladie, M., Rose, J.K., 2006. Sample extraction techniques for enhanced proteomic analysis of plant tissues. Nat. Protoc. 1 (2), 769–774.
Jang, I.C., Yang, J.Y., Seo, H.S., Chua, N.H., 2005. HFR1 is targeted by COP1 E3 ligase for post-translational proteolysis during phytochrome A signaling. Genes Dev. 19 (5), 593–602.
Kim, D.S., Cho, D.S., Park, W.M., Na, H.J., Nam, H.G., 2006. Proteomic pattern-based analyses of light responses in *Arabidopsis thaliana* wild-type and photoreceptor mutants. Proteomics 6 (10), 3040–3049.
Kultima, K., Scholz, B., Alm, H., Skold, K., Svensson, M., Crossman, A.R., Bezard, E., Andren, P.E., Lonnstedt, I., 2006. Normalization and expression changes in predefined sets of proteins using 2D gel electrophoresis: a proteomic study of L-DOPA induced dyskinesia in an animal model of Parkinson's disease using DIGE. BMC Bioinform. 7, 475.
Lastdrager, J., Hanson, J., Smeekens, S., 2014. Sugar signals and the control of plant growth and development. J. Exp. Bot. 65 (3), 799–807.
Lau, O.S., Deng, X.W., 2012. The photomorphogenic repressors COP1 and DET1: 20 years later. Trends Plant Sci. 17 (10), 584–593.
Lee, J., He, K., Stolc, V., Lee, H., Figueroa, P., Gao, Y., Tongprasit, W., Zhao, H., Lee, I., Deng, X.W., 2007. Analysis of transcription factor HY5 genomic binding sites revealed its hierarchical role in light regulation of development. Plant Cell 19 (3), 731–749.
Lopez, L., Carbone, F., Bianco, L., Giuliano, G., Facella, P., Perrotta, G., 2012. Tomato plants overexpressing cryptochrome 2 reveal altered expression of energy and stress-related gene products in response to diurnal cues. Plant Cell Environ. 35 (5), 994–1012.
Mao, J., Zhang, Y.C., Sang, Y., Li, Q.H., Yang, H.Q., 2005. From the cover: a role for *Arabidopsis* cryptochromes and COP1 in the regulation of stomatal opening. Proc. Natl. Acad. Sci. U. S. A. 102 (34), 12270–12275.
Mazzella, M.A., Casal, J.J., 2001. Interactive signalling by phytochromes and cryptochromes generates de-etiolation homeostasis in *Arabidopsis thaliana*. Plant Cell Environ. 24 (2), 155–161.
Mazzella, M.A., Cerdán, P.D., Staneloni, R.J., Casal, J.J., 2001. Hierarchical coupling of phytochromes and cryptochromes reconciles stability and light modulation of *Arabidopsis* development. Development 128 (12), 2291–2299.
Mazzella, M.A., Arana, M.V., Staneloni, R.J., Perelman, S., Rodriguez, B., atiller, M.J., Muschietti, J., Cerdan, P.D., Chen, K., Sanchez, R.A., Zhu, T., Chory, J., Casal, J.J., 2005. Phytochrome control of the *Arabidopsis* transcriptome anticipates seedling exposure to light. Plant Cell 17 (9), 2507–2516.
Minina, E.A., Sanchez-Vera, V., Moschou, P.N., Suarez, M.F., Sundberg, E., Weih, M., Bozhkov, P.V., 2013. Autophagy mediates caloric restriction-induced lifespan extension in *Arabidopsis*. Aging Cell 12 (2), 327–329.
Murchie, E.H., Horton, P., 1997. Acclimation of photosynthesis to irradiance and spectral quality in British plant species: chlorophyll content, photosynthetic capacity and habitat preference. Plant Cell Environ. 20 (4), 438–448.
Osterlund, M.T., Hardtke, C.S., Wei, N., Deng, X.W., 2000. Targeted destabilization of HY5 during light-regulated development of *Arabidopsis*. Nature 405 (6785), 462–466.
Oyama, T., Shimura, Y., Okada, K., 1997. The *Arabidopsis* HY5 gene encodes a bZIP protein that regulates stimulus-induced development of root and hypocotyl. Genes Dev. 11 (22), 2983–2995.
Peschke, F., Kretsch, T., 2011. Genome-wide analysis of light-dependent transcript accumulation patterns during early stages of *Arabidopsis* seedling deetiolation. Plant Physiol. 155 (3), 1353–1366.
Phee, B.K., Park, S., Cho, J.H., Jeon, J.S., Bhoo, S.H., Hahn, T.R., 2007. Comparative proteomic analysis of blue light signaling components in the *Arabidopsis* cryptochrome 1 mutant. Mol. Cells 23 (2), 154–160.
Pogson, B.J., Woo, N.S., Forster, B., Small, I.D., 2008. Plastid signalling to the nucleus and beyond. Trends Plant Sci. 13 (11), 602–609.
Pogson, B.J., Albrecht, V., 2011. Genetic dissection of chloroplast biogenesis and development: an overview. Plant Physiol. 155 (4), 1545–1551.
Quail, P.H., Boylan, M.T., Parks, B.M., Short, T.W., Xu, Y., Wagner, D., 1995. Phytochromes photosensory perception and signal transduction. Science 268 (5211), 675–680.
Ruckle, M.E., Burgoon, L.D., Lawrence, L.A., Sinkler, C.A., Larkin, R.M., 2012. Plastids are major regulators of light signaling in *Arabidopsis thaliana*. Plant Physiol.
Seo, H.S., Yang, J.Y., Ishikawa, M., Bolle, C., Ballesteros, M.L., Chua, N.H., 2003. LAF1 ubiquitination by COP1 controls photomorphogenesis and is stimulated by SPA1. Nature 423 (6943), 995–999.
Sharkey, T.D., Bernacchi, C.J., Farquhar, G.D., Singsaas, E.L., 2007. Fitting photosynthetic carbon dioxide response curves for C(3) leaves. Plant Cell Environ. 30 (9), 1035–1040.
Shen, H., Zhu, L., Castillon, A., Majee, M., Downie, B., Huq, E., 2008. Light-Induced phosphorylation and degradation of the negative regulator phytochrome-interacting factor1 from *Arabidopsis* depend upon its direct physical interactions with photoactivated phytochromes. Plant Cell 20 (6), 1586–1602.
Shin, J., Kim, K., Kang, H., Zulfugarov, I.S., Bae, G., Lee, C.H., Lee, D., Choi, G., 2009. Phytochromes promote seedling light responses by inhibiting four negatively-acting phytochrome-interacting factors. Proc. Natl. Acad. Sci. U. S. A. 106 (18), 7660–7665.
Smyth, G.K., 2004. Linear models and empirical bayes methods for assessing differential expression in microarray experiments. Stat. Appl. Genet. Mol. Biol. 3 (1), 1–25.
Smyth, G.K., 2005. Limma Linear Models for Microarray Data. Bioinformatics and Computational Biology Solutions Using R and Bioconductor. In: Gentleman, R., Carey, V.J., Huber, W., Irizarry, R.A., Dudoit, S. (Eds.). Springer, New York, pp. 397–420.
Strasser, B., Sanchez-Lamas, M., Yanovsky, M.J., Casal, J.J., Cerdan, P.D., 2010. *Arabidopsis thaliana* life without phytochromes. Proc. Natl. Acad. Sci. U. S. A. 107 (10), 4776–4781.
Wang, F.-F., Lian, H.-L., Kang, C.-Y., Yang, H.-Q., 2010. Phytochrome B is involved in mediating red light-induced stomatal opening in *Arabidopsis thaliana*. Mol. Plant 3 (1), 246–259.
Xu, L., i, Y., uejun, Y., ang, Y.L., Jie, W., ang, X., iaoJuan, X., iao ea, 2009. Protein identification and mRNA analysis of phytochrome-regulated genes in *Arabidopsis* under red light. Sci. China C Life Sci. 52 (4).
Yang, Y.J., Zuo, Z.C., Zhao, X.Y., Li, X., Klejnot, J., Li, Y., Chen, P., Liang, S.P., Yu, X.H., Liu, X.M., Lin, C.T., 2008. Blue-light-independent activity of *Arabidopsis* cryptochromes in the regulation of steady-state levels of protein and mRNA expression. Mol Plant 1 (1), 167–177.
Zivcak, M., Brestic, M., Kalaji, H.M., Govindjee, 2014. Photosynthetic responses of sun- and shade-grown barley leaves to high light: is the lower PSII connectivity in shade leaves associated with protection against excess of light? Photosynth Res. 119 (3), 339–354.